Rod-shaped bismuth oxyiodide as a novel anode material for sodium-ion batteries

Jiaju Lu[ab], Weiya Tian[ab], Xiaoling Wang [ab], Zheng Xu [ab], Tengfei Li [ab], Junxian Hu* [ab], Puqiang He*[c] and Yaochun Yao* [ab]

[a]*National Engineering Research Center of Vacuum Metallurgy, Kunming, China*

[b]*Faculty of Metallurgy and Energy Engineering, Kunming University of Science and Technology, Kunming, China*

[c]*Xinjiang Production & Construction Corps Key Laboratory of Green and Intelligent Development and Efficient Utilization of Strategic Mineral Resources, Xinjiang University of Technology, Hotan, China*

***Correspondence**:* Junxian Hu (hujunxian@kust.edu.cn)

Puqiang He (270905839@qq.com)

Yaochun Yao (yaochun9796@163.com)

Experimental section

1.Material Preparation

First, 0.97 g of $Bi(NO_3)_3 \cdot 5H_2O$ was weighed and dissolved in 60 mL of deionized water, and the mixture was stirred for 30 minutes. Then, 30 mL of 1.5 mol/L NaOH solution was added and stirred to form a mixture. Next, 0.996 g of KI was weighed and dissolved in 30 mL of deionized water, and the mixture was stirred until completely dissolved. The KI solution was then slowly added to the mixture and stirred for 60 minutes. The mixture was transferred to a 200 mL high-pressure reactor and reacted at 180 °C for 24 hours. Finally, it was dried in an oven at 60 °C for 12 hours to obtain

B_5O_7I.

2 Material Characterizations

The morphological characteristics of B_5O_7I was detected by ZEISS Sigma 300 SEM. The detailed structures and elemental distributions were characterized using a JEM-1400 flash lamp and a JEOL 2100 F mission electron microscope (TEM, 200 kV). XRD tests were conducted using Cu-Kα rays on a Rigaku Miniflex 600 diffractometer. XPS tests were completed on the Thermo Scientific K-Alpha+ system.

3 Electrochemical Measurements

After grinding the electrode material, Super P and polyvinylidene fluoride (PVDF) in a mass ratio of 7:2:1, N-methyl pyrrolidine (NMP) was added to form a uniform slurry, which was then coated onto the surface of the copper foil. A B_5O_7I electrode with a diameter of 10 mm and a loading capacity of approximately 2.5 mg cm^{-2} was obtained. Then, the electrodes were assembled into coin cells (CR 2025) using glass fiber (Whatman GF/D) membranes and electrolyte (1 M $NaPF_6$ in DME) in an argon-filled glove box (with O_2 and H_2O content below 0.1 ppm). Electrolyte amount: For each CR2025 coin cell, 120 μL of 1 M $NaPF_6$ in DME electrolyte was used. Cyclic voltammogram (CV) measurements were carried out using an IviumStat Vertex. One. EIS electrochemical workstation at different scanning rates. The galvanostatic charge-discharge (GCD) curves were recorded at different current densities using the LAND-CT 3002A test system.

GITT was investigated with a pulse current of 200 mA g^{-1} for 20 min, followed by a rest interval for 40 min. The following equation is applied to calculate the diffusion

coefficient:

$$D_K = \frac{4}{\pi}\left(\frac{m_B V_M}{M_B S}\right)\left(\frac{\Delta E_S}{\Delta E_\tau}\right)^2$$

where τ is the constant current pulse duration, m_B, M_B, and V_M are the mass, molar mass, and molar volume of the active material, S is the electrode/electrolyte contact area, and ΔE_s and ΔE_τ are the steady-state voltage change and the voltage change during the pulse, respectively.

Table 1. Element composition test.

Element	Content (%)
Bi	81.47%
O	8.8%

$$I(wt\%) = 1 - 81.47\% - 8.8\% = 9.73$$

$$Bi{:}O{:}I = \frac{81.47\%}{209}:\frac{8.8\%}{16}:\frac{9.73\%}{126.9} = 5.08{:}7.17{:}1$$

Theoretical content of each element in Bi_5O_7I

$$Bi(wt\%) = \frac{5 \times M_{Bi}}{M_{Bi_5O_7I}} = \frac{5 \times 209}{1283.9} = 81.39\%$$

$$O(wt\%) = \frac{7 \times M_O}{M_{Bi_5O_7I}} = \frac{7 \times 16}{1283.9} = 8.72\%$$

$$I(wt\%) = \frac{M_I}{M_{Bi_5O_7I}} = \frac{126.9}{1283.9} = 9.89\%$$

Theoretical content of each element in BiOI

$$Bi(wt\%) = \frac{M_{Bi}}{M_{BiOI}} = \frac{209}{351.9} = 59.39\%$$

$$O(wt\%) = \frac{M_O}{M_{BiOI}} = \frac{16}{351.9} = 4.55\%$$

$$I(wt\%) = \frac{M_I}{M_{BiOI}} = \frac{126.9}{351.9} = 36.06\%$$

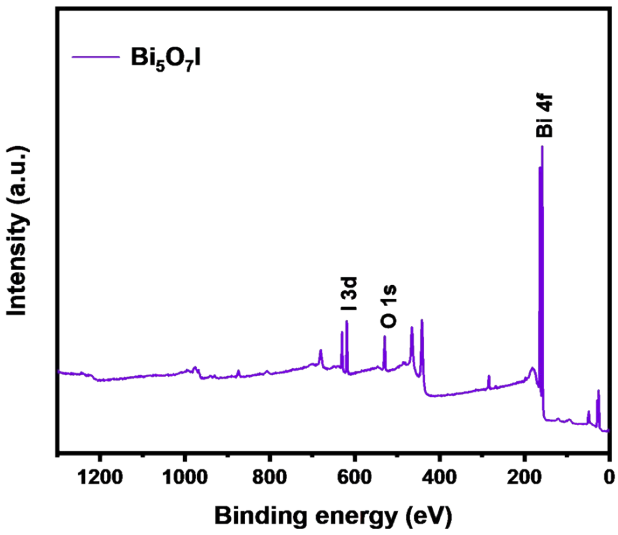

Fig. S1 Total XPS graph of Bi_5O_7I sample.

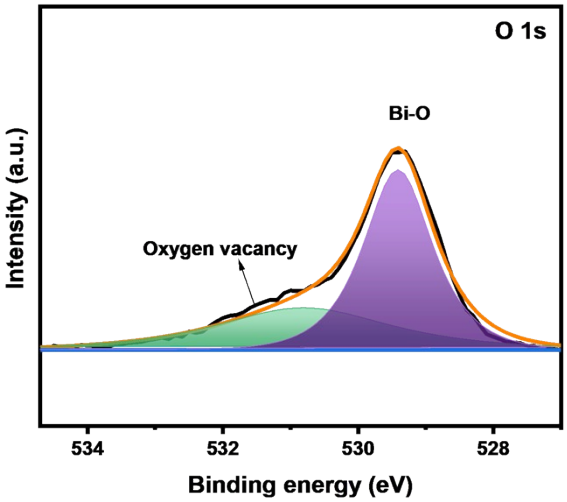

Fig. S2 O 1s XPS spectra of Bi_5O_7I sample.

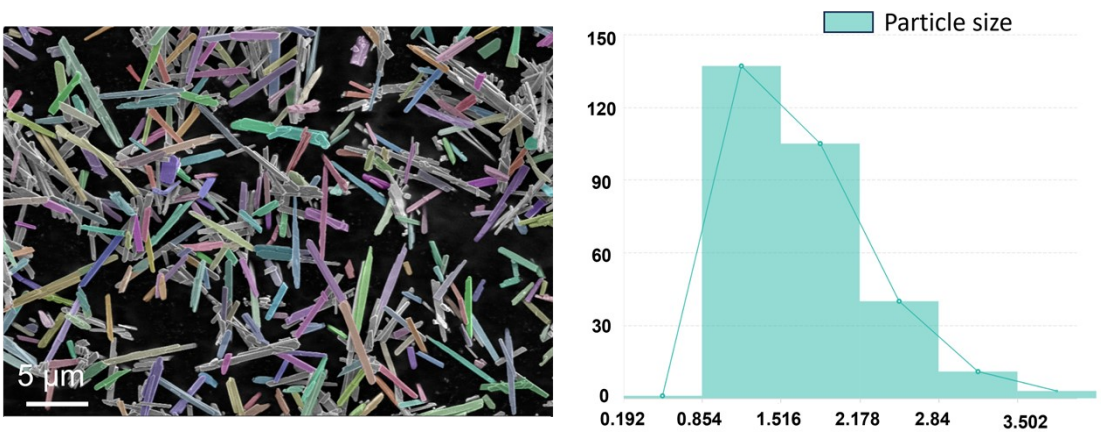

Fig. S3 Statistical size distribution histogram of Bi_5O_7I microrods.

Table S2. Particle size data statistics table.

X-axis - Particle size range	Y-axis - Number of Particles
[0.192,0.854)	1
[0.854,1.516)	137
[1.516,2.178)	105
[2.178,2.84)	40
[2.84,3.502)	11
[3.502,4.164]	3
/	297

Table S3. Particle size information.

Average particle size	Particle size standard deviation
1.694μm	0.563μm

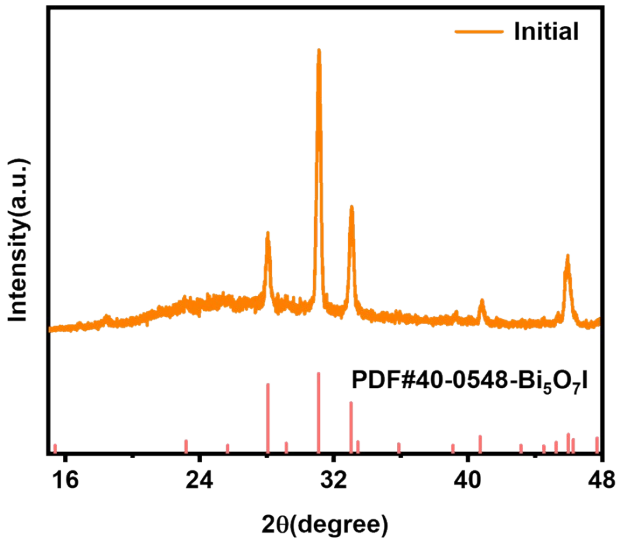

Fig. S4 The in situ XRD pattern of the Bi_5O_7I electrode at the initial stage.

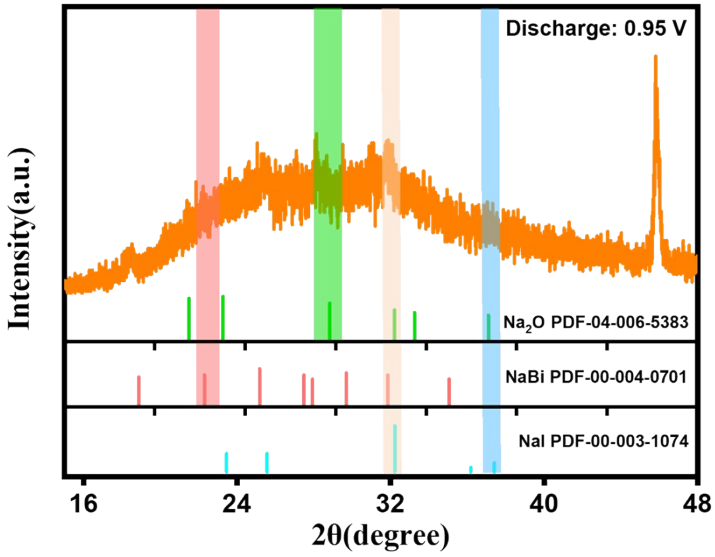

Fig. S5 The in situ XRD pattern of the Bi_5O_7I electrode when the discharge voltage reached 0.95V.

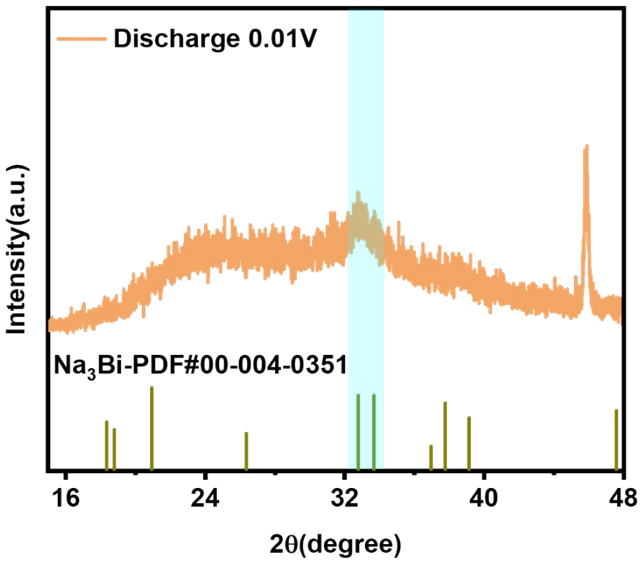

Fig. S6 The in situ XRD pattern of the Bi_5O_7I electrode when the discharge voltage reached 0.01V.

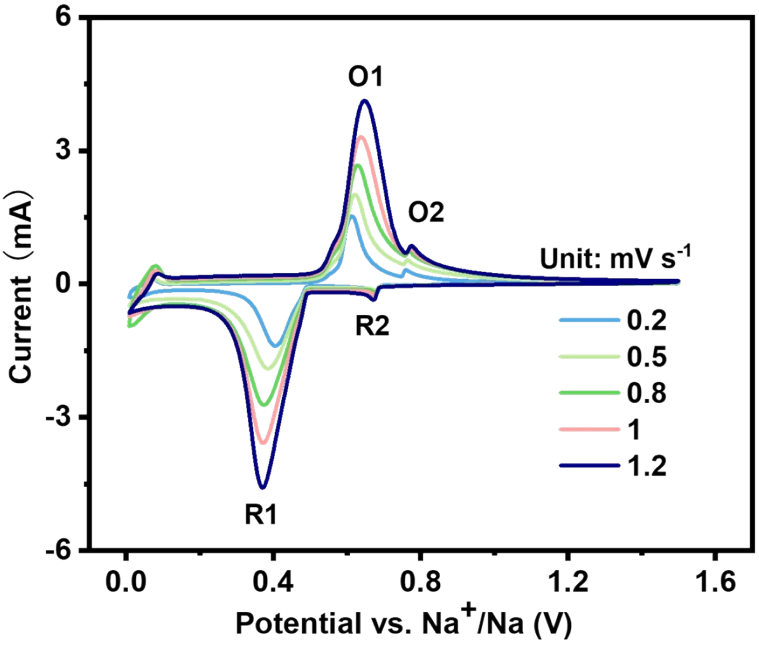

Fig. S7 CV curves of Bi_5O_7I electrode at 0.2 to 1.2 mV s^{-1}.

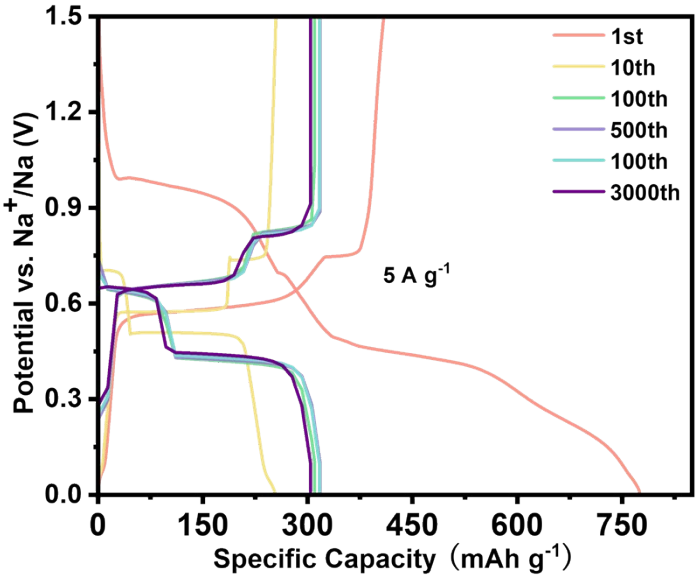

Fig. S8 Discharge/charge profiles of Bi_5O_7I electrode at 5 A g^{-1}.

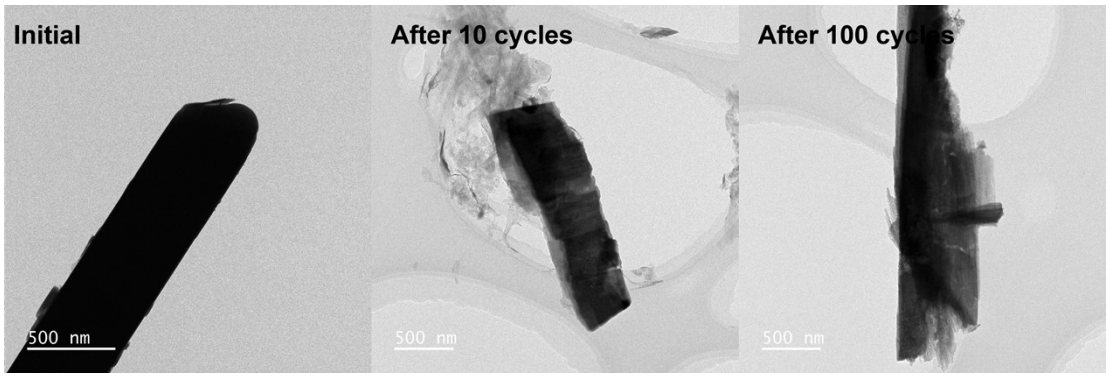

Fig. S9 TEM images of the Bi_5O_7I electrode under different number of cycles.

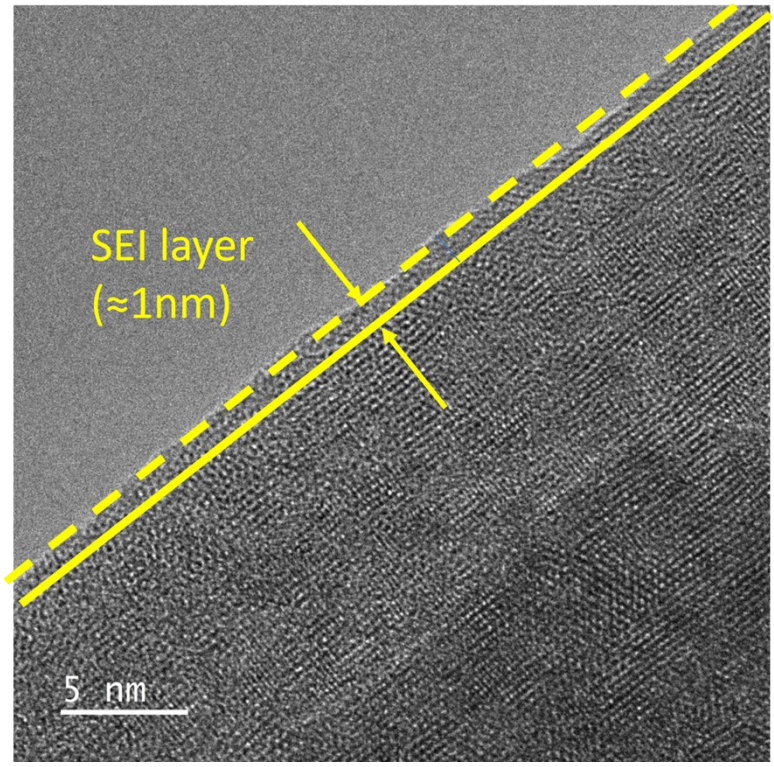

Fig. S10 The SEI of Bi_5O_7I electrode.

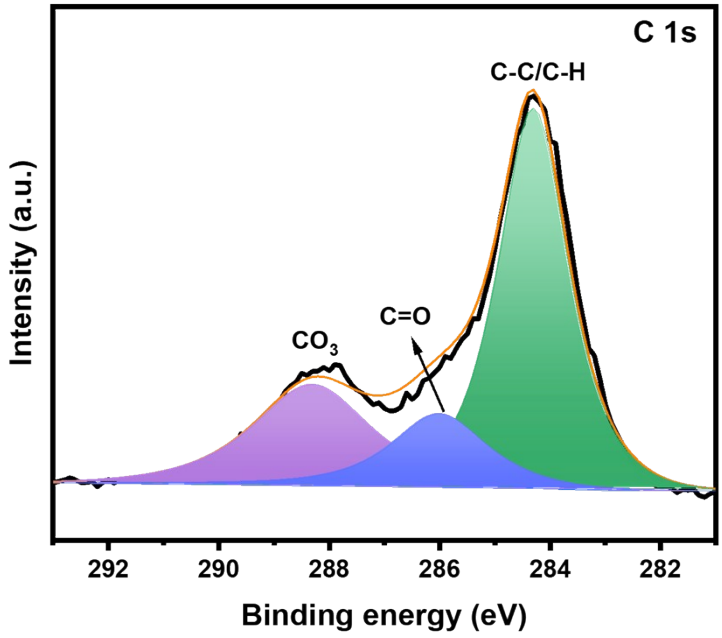

Fig. S11 C 1s XPS of Bi_5O_7I electrode.

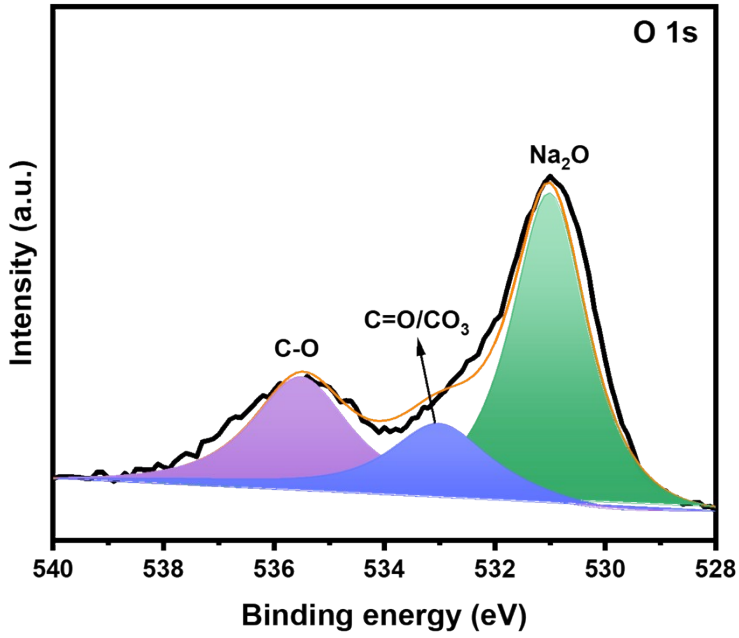

Fig. S12 O 1s XPS of Bi_5O_7I electrode.

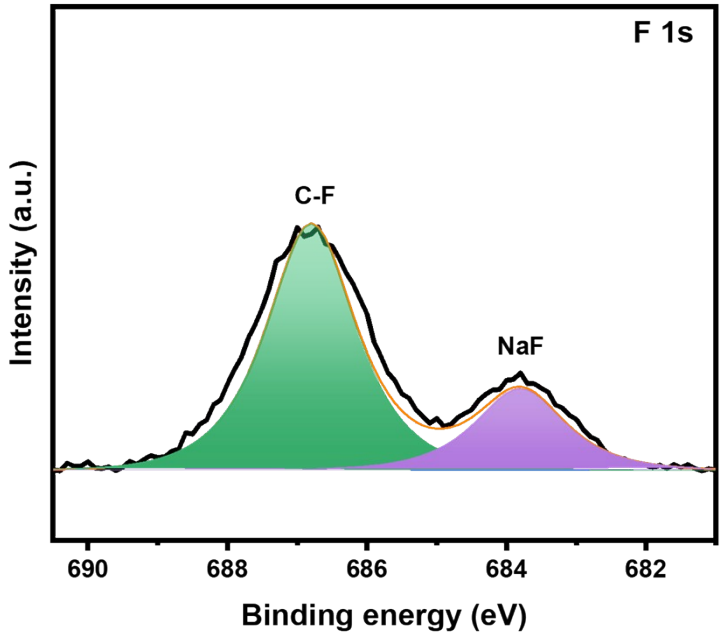

Fig. S13 F 1s XPS of Bi_5O_7I electrode.

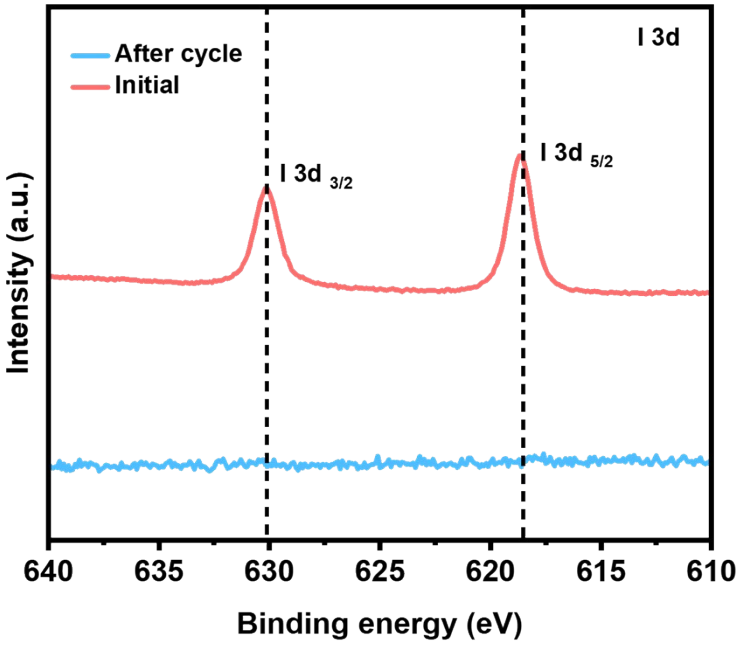

Fig. S14 I 3d XPS of Bi_5O_7I electrode.

Table S4 Comparison of Bi_5O_7I electrodes with other alloy anodes in recent years.

Materials	Specific capacity (mAh/g)	Cycle	Current density (A/g)	Ref
Bi_5O_7I	292.6	3000	5	This work
UTP BiOCl NSs	~200	3000	5	[1]
Bi_2Se_3@rGO@NC	94.0	1000	0.2	[2]
Bi_2S_3/Sb_2S_3	369.4	500	1	[3]
$Bi_2S_{3-x}Se_x$@rGO	701	100	0.1	[4]
Bi_2Se_3@NC	238	500	5	[5]

References

[1] S.-L. Wei, Y.-L. Yang, X.-L. Shi, Y. Sun, J.-G. Chen, X.-F. Tian, Y.-T. Wu, Z.-G. Chen, Chem. Eng. J., 2024, 489, 151346.
[2] S. Chong, L. Yuan, S. Qiao, M. Ma, T. Li, X.L. Huang, Q. Zhou, Y. Wang, W. Huang, Sci. China Mater. 2023, 66, 2641-2651.
[3] Y. Dong, B. Murugesan, W. Lin, C. Wang, J. Dai, W. Li, Q. Ma, X. Yang, Y. Cai, Ionics,2024, 30, 4043-4053.
[4] M. Han, Y. Xi, S. Luan, J. Zhou, F. Gao, Mater. Chem. Phys., 2022, 292, 126806.
[5] X. Liu, S. Zhang, Z. Duan, X. Guo, Y. Liu, X. Zheng, Q. Fan, Q. Kong, J. Zhang, J. Power Sources,2025, 649, 237471.